LEGIBILITY NOTICE

1

LA-UR -89-2430

LA-UR--89-2430

DE89 015251

Los Alamos National Laboratory is operated by the University of California for the United States Department of Energy under contract W-7405-ENG-36.

TITLE: NUMERICAL SIMULATION OF WAVE PROPAGATION THROUGH CEMENTED GRANULAR MATERIAL

AUTHOR(S): Bruce C. Trent

SUBMITTED TO: A.S.M.E. International Symposium on Wave Propagation in Granular Media, San Francisco, CA, December 10-14, 1989.

Los Alamos

Los Alamos National Laboratory
Los Alamos, New Mexico 87545

Numerical Simulation of Wave Propagation Through Cemented Granular Material

Bruce C. Trent
Los Alamos National Laboratory
Los Alamos, NM 87545

ABSTRACT

The distinct element method (DEM) has been used to model wave propagation through a matrix material composed of circular particles which are glued together with elastic bonds. Wave propagation through the sample is shown to be governed by the properties and distribution of individual bonds.

NOMENCLATURE

a - separation parameter $(1 + \delta)$
c - fracture length for growth criterion (mm)
E - elastic modulus of bonding material (MPa)
F - restoring force of bond on particle (N)
R - particle radius (mm)
T - surface energy (MPa-mm)
Δu - incremental stretching of bond (mm)
α - dimensionless length of bond (see Fig. 1)
β - dimensionless length of crack (see Fig. 1)
δ - dimensionless width of bond (see Fig. 1)
ν - Poisson's ratio of bonding material
σ_n - normal stress in bond (MPa)
σ_s - shear stress in bond (MPa)

INTRODUCTION

The distinct element code used is SKRUBAL. It was modified from the TRUBAL program (Cundall, 1987) by allowing pairs of particles to be bonded together by an elastic material, as shown in Fig. 1. The details of the formulation are presented elsewhere (Trent, 1987). Three modes of relative motion were analyzed for the two-dimensional case presented here: simple tension, where the particles move in the direction of a line connecting their centers; rolling torsion, where the particles rotate in opposite directions; and shearing torsion where the particles rotate in the same direction. Any arbitrary motion of two particles may be decomposed into these three components plus rigid body motion. The form of the restoring forces in simple tension is:

$$\frac{F/\Delta u}{E} =$$

$$-w + \frac{a}{\sqrt{a^2-1}}\arccos\left(\frac{a\cos(w)-1}{a-\cos(w)}\right)\Bigg|\begin{matrix} w=\sin^{-1}(\alpha) \\ w=\sin^{-1}(\beta)\end{matrix} \quad . \qquad (1)$$

Analytic expressions such as this are incorporated into the calculational sequence of the distinct element code so that bonded particles have forces and moments applied to them in addition to those imposed by particle- particle interactions.

The bond behaves elastically until the stresses in the material exceed a critical value. Specifically, a generalized Griffith criterion (Margolin, 1984) was modified so that fracture occurs when:

$$\sigma_n^2 + \frac{\sigma_s^2}{2(1+\nu)} \geq \frac{\pi T E}{2(1-\nu^2)c} \quad . \qquad (2)$$

The calculations presented in this paper have two important features. First, none of the particles were initially touching, so that all particle interaction results only from forces and moments generated in the bonding. This means that all the mass of the sample is concentrated in the particles while all the stiffness is in the bonding. Secondly, although bonds are examined with different initial damage, fracture growth is not allowed to further deteriorate any bond. The scope of this particular research is to show how the macroscopic longitudinal wave velocity is influenced by the elastic properties of the bonding material, the initial damage of those bonds, and the topology of bonded particles.

NUMERICAL EXPERIMENTS

Figure 2 shows the initial particle assembly. Each particle has a radius of 1 mm and no two particles are touching. Bonds were then established for any pair of particles separated by less than 0.25 mm. The shaded areas identify six regions where particle velocities are averaged and plotted as time histories. The sample is loaded by specifying a 10 m/s tensile (downward) velocity for a short time on the lowermost 20 particles. This motion is transferred to the rest of the assembly through the bonding. Bonds are represented in Fig. 2 by lines connecting particle centers. Notice that there is an unattached particle near the center of velocity region 6. Also, a cluster of three particles is detached from the rest of the assembly. Each bond is assumed to be 95 percent intact ($\beta/\alpha = 0.05$) throughout the calculation. Notice from Eq. 1 that the force-displacement relation is strongly dependent upon the initial separation, $2\delta R$, so that although each bond has the same fracture length, thin bonds are much stiffer than thicker ones.

A second sample is shown in Fig. 3. It is identical to Fig. 2, except that all particles within one half particle radius (0.5 mm) are bonded together. The vertical boundaries are periodic so bonds exist there, connecting the two sides, but they are not illustrated in Figs. 2 and 3.

Influence of Bond Stiffness on Damped Response

The input boundary condition to the assembly in Fig. 2 is shown in Fig. 4 as a square wave. The other five curves represent the average velocity of all particles within a given region. Numerical damping was applied to the equations of motion in order to study the behavior during relaxation. The mass and stiffness proportional damping is discussed by Strack and Cundall (1978). The highest velocities are in region 6, adjacent to the free surface. The elastic modulus of the bonds in this calculation was 55 MPa, typical of a stiff limestone.

Snapshots of the vertical velocity of each particle at various times are shown in Figs. 5a to 5f. The "at rest" condition is shown in Fig. 5a. Midway through the applied velocity condition, each particle is moving downward as shown in Fig. 5b, except for those four particles near the top of the assembly which are completely detached from the other particles. The particle velocities at the final cycle of the imposed condition are given in Fig. 5c. Notice that most of the particles are now moving downward faster than the boundary as a compressive wave has been formed due to the free surface at the top of the sample. In Fig. 5d to 5f the lower particles are at rest and the others slow down due to the applied damping.

The family of velocity time histories in Fig. 6 show a much softer response to the identical loading of the assembly shown in Fig. 2. The bonds in this experiment had an elastic modulus of 1 GPa. The snapshots in Figs. 7a to 7f are at identical times as those in Fig. 5. Notice that at the end of the imposed velocity (Fig. 7c) one half of the particles are not yet moving. The particles come to rest much more slowly, as shown in Fig. 7f, where most of the particles are still moving downward.

Microscopic Influence on Wave Propagation

An elastic modulus of 20 GPa was assigned to the bonds shown in Fig. 2. No damping was applied to the particles and the resulting harmonic response is shown in Fig. 8. The total length of the sample is 32 mm. The wave must then travel a total of 64 mm for a complete tension/compression cycle. The average time required for this transit is obtained by dividing by three, the total time for three complete cycles (158 - 26) μsec. The resulting mean wave speed through the sample is thereby 1460 m/s, which is typical of alluvium, a cemented granular material.

Figure 9 shows how the energy in the system changes from translational kinetic energy in the particles to strain energy in each of the three modes of deformation in the bonding. The lower curve is rotational kinetic energy in the particles which rises to a low level and is thereafter insensitive to the sample ringing. The total energy curve shows a small but sharp drop as the lower boundary particles are stopped. The slight oscillation in amplitude is due to forcing those boundary particles to be fixed, i.e. the energy required to hold those particles fixed is not accounted for in Fig. 9.

The elastic modulus of the bonding material was reduced by a factor of two to a value of 10 GPa. The corresponding longitudinal wave speed taken from Fig. 10 is 1050 m/s. The sound speed of a homogeneous elastic material is

$$c_\ell = \sqrt{\frac{E\ \ (1-\nu)}{(1+\nu)(1-2\nu)\rho}} \quad . \tag{3}$$

The measured reduction of 1.39 is very nearly equal to the square root of two, indicating the macroscopic sound speed is governed by the elasticity of the bonding material only. A material with a density of 2400 kg/m^3, Poisson's ratio of 0.18, and elastic modulus of 20 GPa has a sound speed of 3008 m/s, or 2.06 times the value measured in Fig. 8. This is not surprising, given the relatively small number of bonds that are present.

If the extent of bonding is different prior to loading, the response is significantly different. A much stiffer response was observed due to the 83 additional bonds that were generated by allowing those particles whose separation was between 0.25 and 0.50 mm to be connected. Fig. 11 shows an increased wave speed of 1440 m/s, even with the lower elastic modulus of 10 GPa.

Equation 1 shows the dependence of the bond restoring force on fracture length. All the bonds in the calculations presented thus far has fractures that were only 5 percent of the total bond length. This was increased to 20 percent and the macroscopic sound speed once again drops. Figure 12 shows the response and the sound speed obtained from this plot was 1150 m/s.

SUMMARY

Several calculations have been presented that were performed with the bonded distinct element code, SKRUBAL. The results show that macroscopic sound speed is greatly influenced by the microstructure. Specifically, the longitudinal sound speed varies with the elastic modulus of the bonding material, the number of particles that are bonded together, and the initial fracture lengths within the individual bonds.

REFERENCES

Cundall, P.A., 1987, "Distinct Element Models of Rock and Soil Structure," ***Analytical and Computational Methods in Engineering Rock Mechanics***, E.T. Brown, ed., Allen & Unwin, London, pp. 129-163.

Margolin, L.G., 1984, "Generalized Griffith Criterion for Crack Propagation," ***Engineering Fracture Mechanics***, Vol. 19, pp. 539-543.

Strack, O.D.L. and Cundall, P.A., 1978, "The Distinct Element Method as a Tool for Research in Granular Media," Report to the National Science Foundation, NSF Grant ENG76-20711, Part I, Appendix 1, pp 24-26.

Trent, B.C., 1987, "The Effect of Micro-Structure on the Macroscopic Behavior of Cemented Granular Material," Ph.D. Thesis, University of Minnesota, Minneapolis, MN.

This work performed under the auspices of the U.S. Department of Energy.

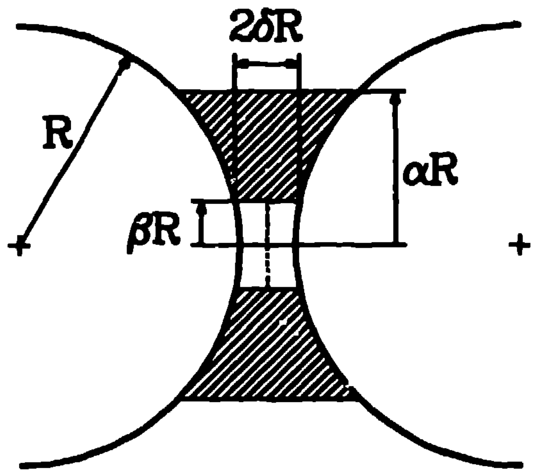

Fig. 1. Assumed shape of elastic bonding material, defined by three dimensionless values.

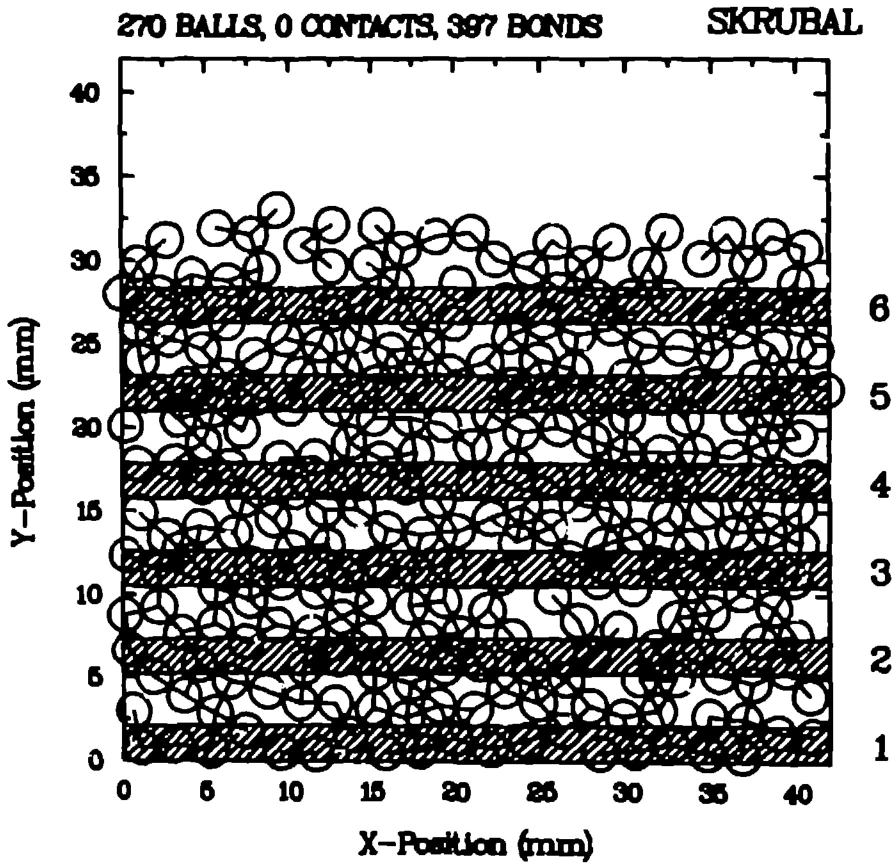

Fig. 2. Assembly of particles and bonds. Shaded areas are regions where particle velocities are averaged for time histories. All particles within 0.25 mm (R/4) are bonded together, as represented by the straight lines.

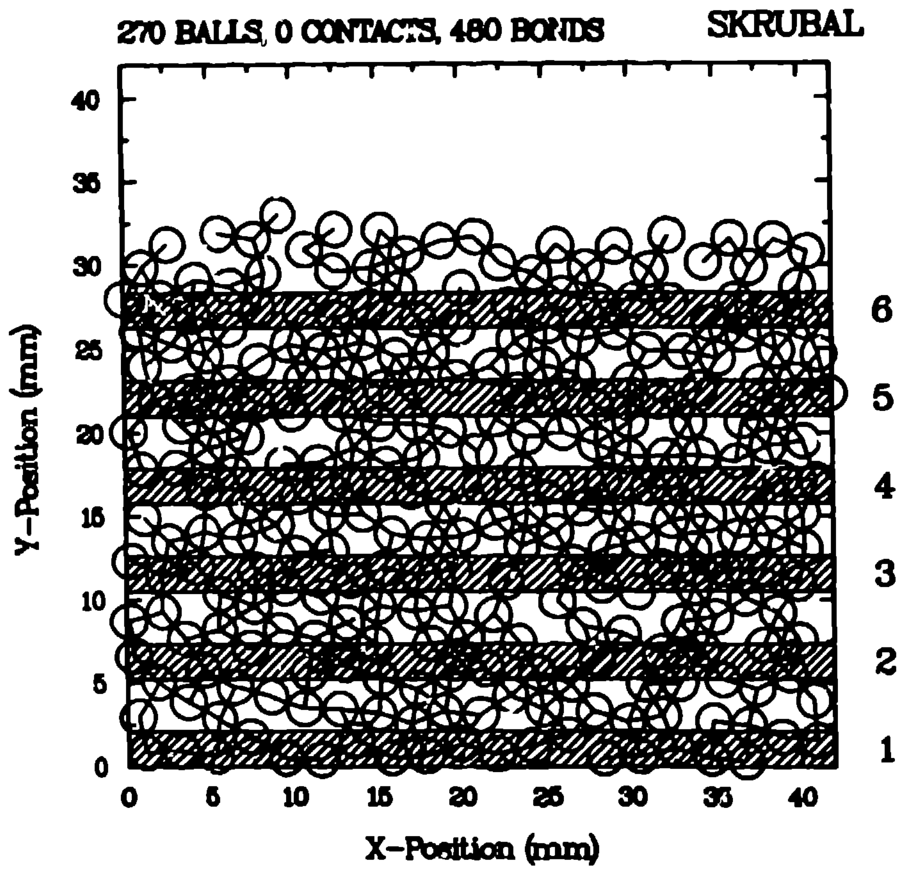

Fig. 3. 83 additional bonds are generated as particles within 0.5 mm (R/2) are bonded together.

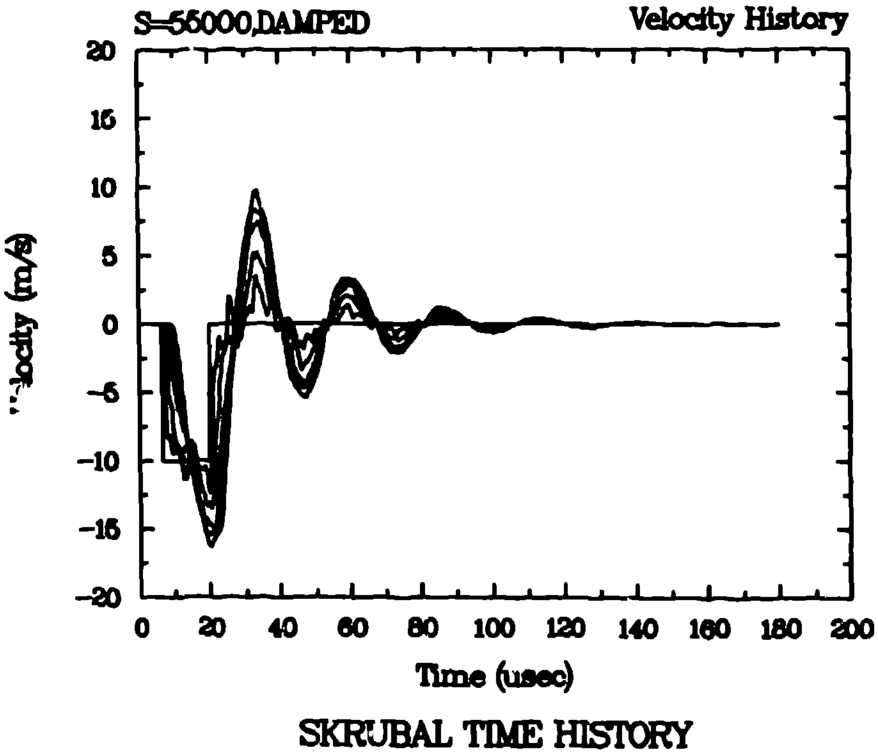

Fig. 4. Damped wave propagation through the sample in Fig. 2, assuming an elastic modulus of 55 GPa and bonds that are 95% intact. The different curves represent the average velocities for the six regions shown in Figs. 2 and 3.

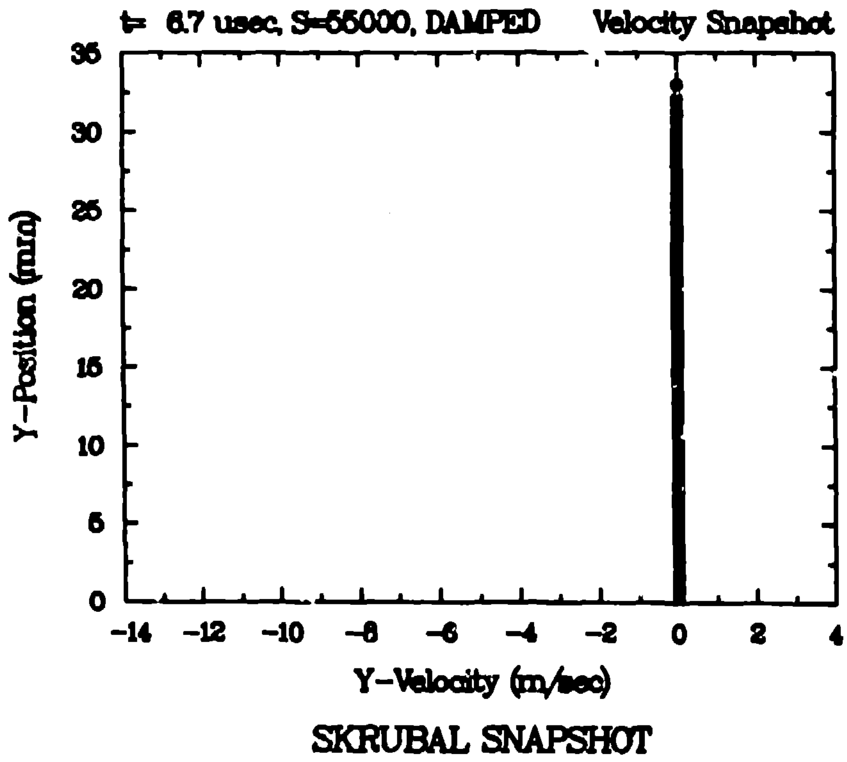

Fig. 5a.

Fig. 5a-f. Vertical velocities for all particles at various times during the loading depicted in Fig. 4. Notice the rapid response as the boundary particles are moved.

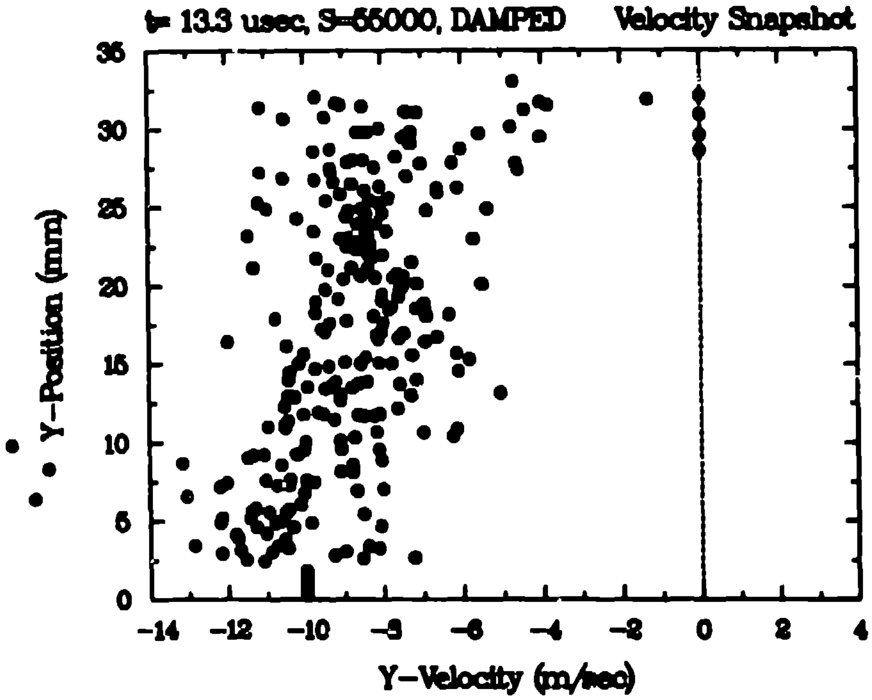

SKRUBAL SNAPSHOT

Fig. 5b.

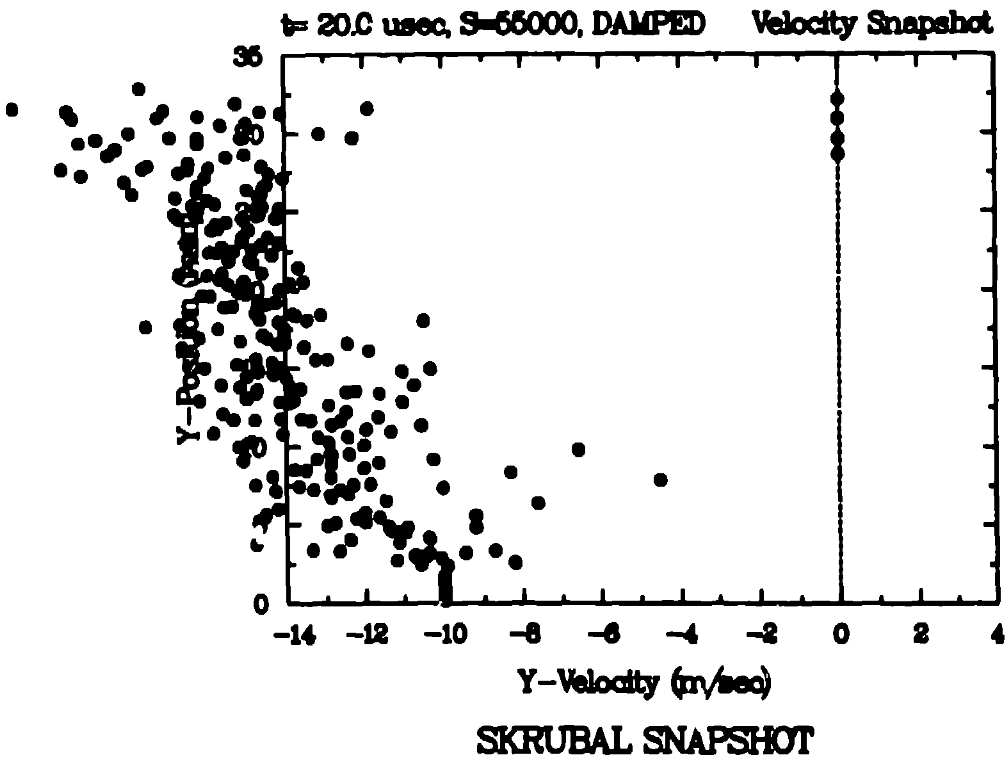
t= 20.0 usec, S=55000, DAMPED Velocity Snapshot
Y-Velocity (m/sec)
Y-Position
SKRUBAL SNAPSHOT

Fig. 5c.

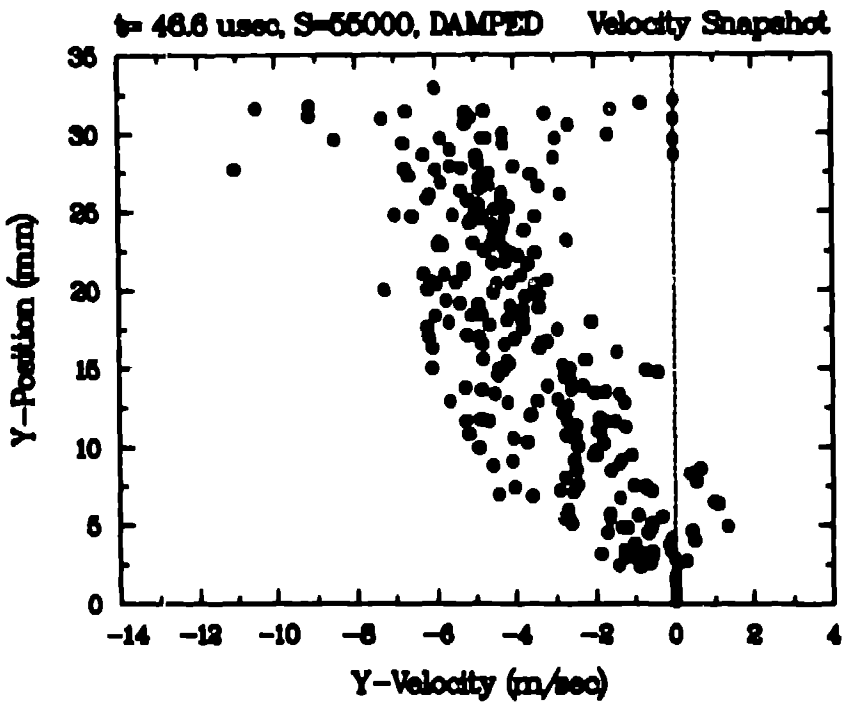

SKRUBAL SNAPSHUT

Fig. 5d.

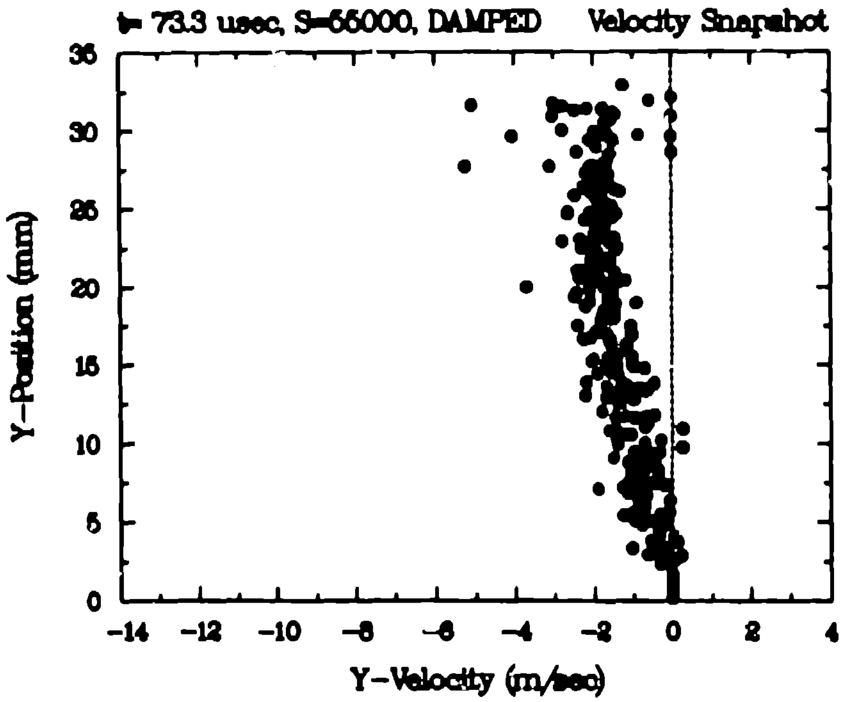

SKRUBAL SNAPSHOT

Fig. 5e.

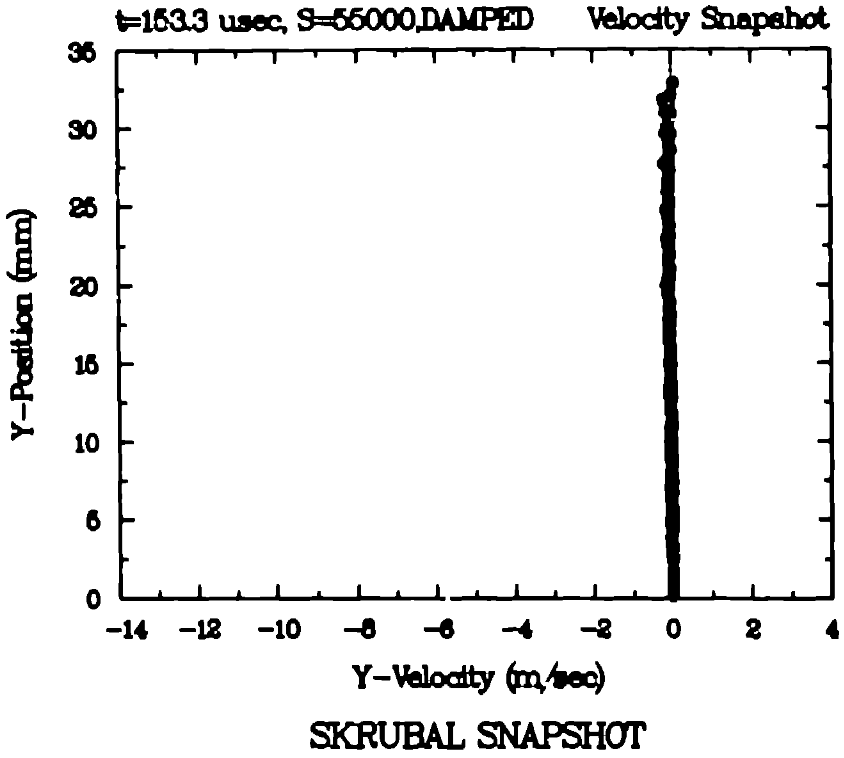
t=153.3 usec, S=55000,DAMPED
Velocity Snapshot
Y-Position (mm)
35
30
25
20
15
10
5
0
-14
-12
-10
-8
-6
-4
-2
0
2
4
Y-Velocity (m/sec)
SKRUBAL SNAPSHOT

Fig. 5f.

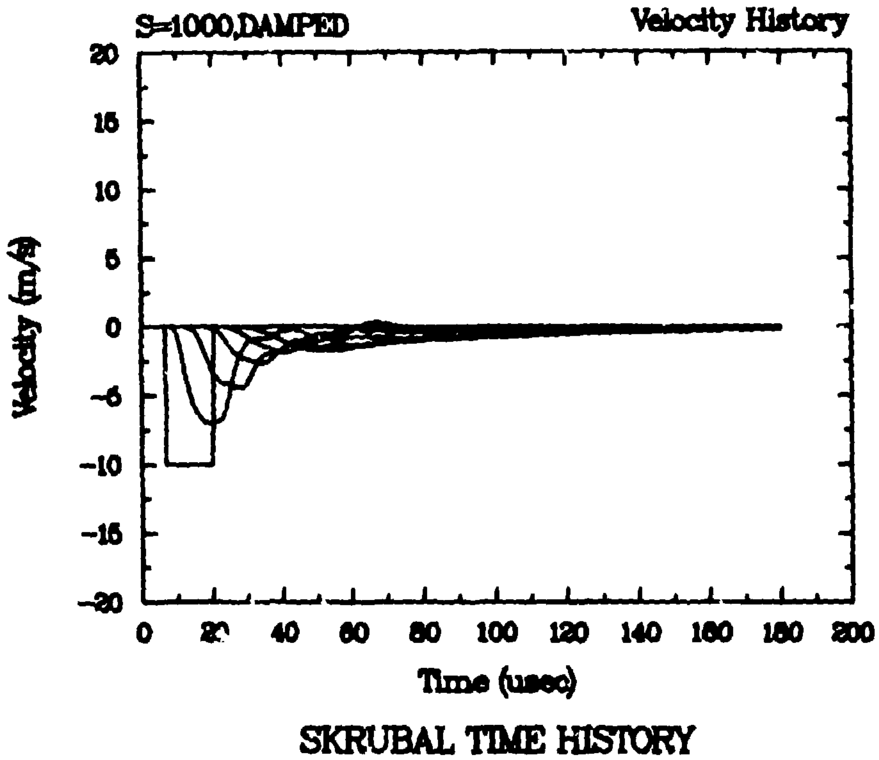

Fig. 6. Damped wave propagation through the sample in Fig. 2, assuming a much softer elastic modulus of 1 GPa. Bonds are 95% intact.

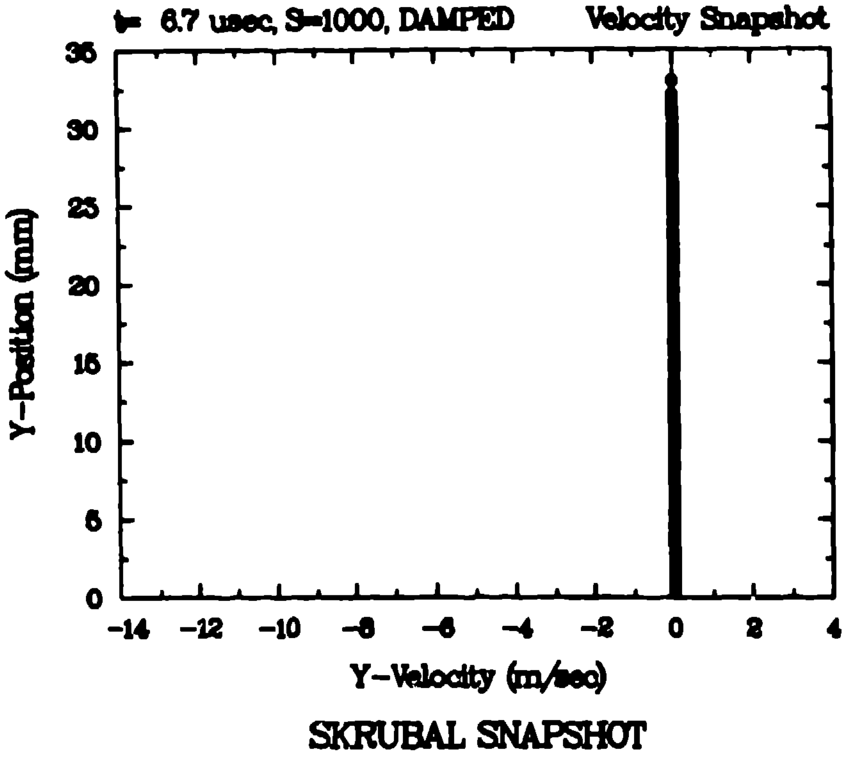

Fig. 7a.

Fig. 7a-f. Vertical velocities for all particles at various times during the loading depicted in Fig. 4. Notice the sluggish response.

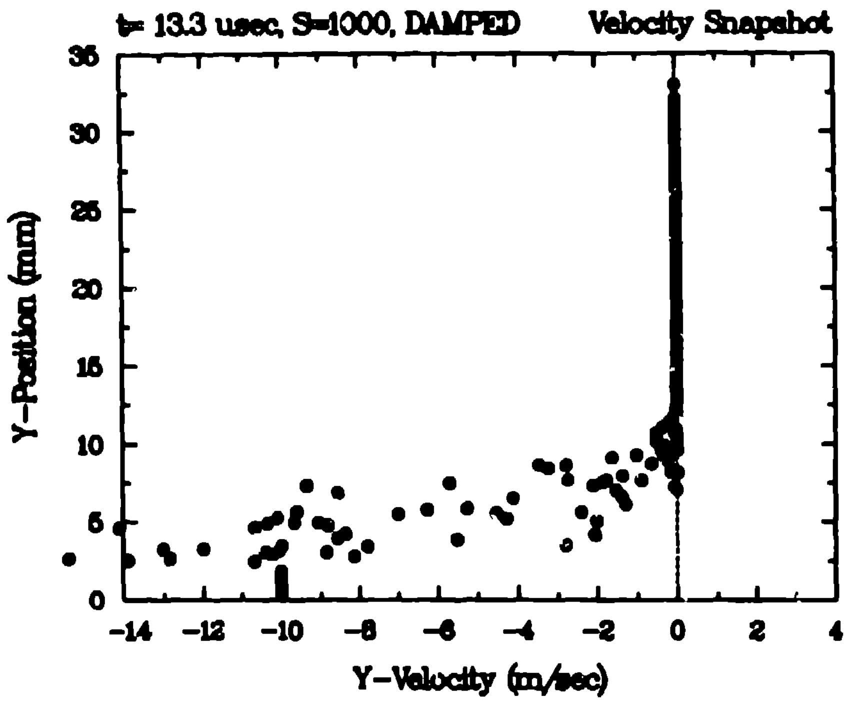

SKRUBAL SNAPSHOT

Fig. 7b.

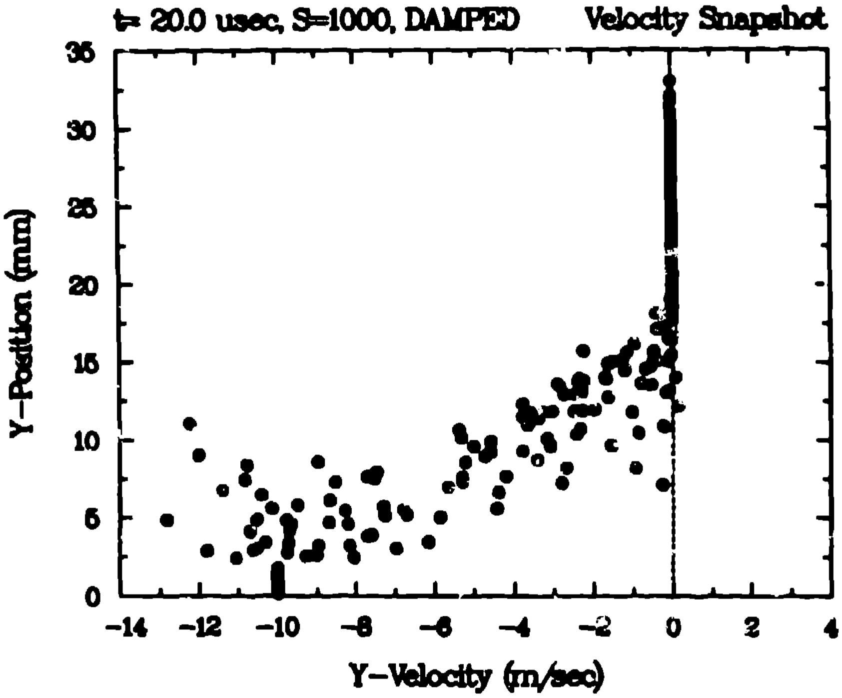

SKRUBAL SNAPSHOT

Fig. 7c.

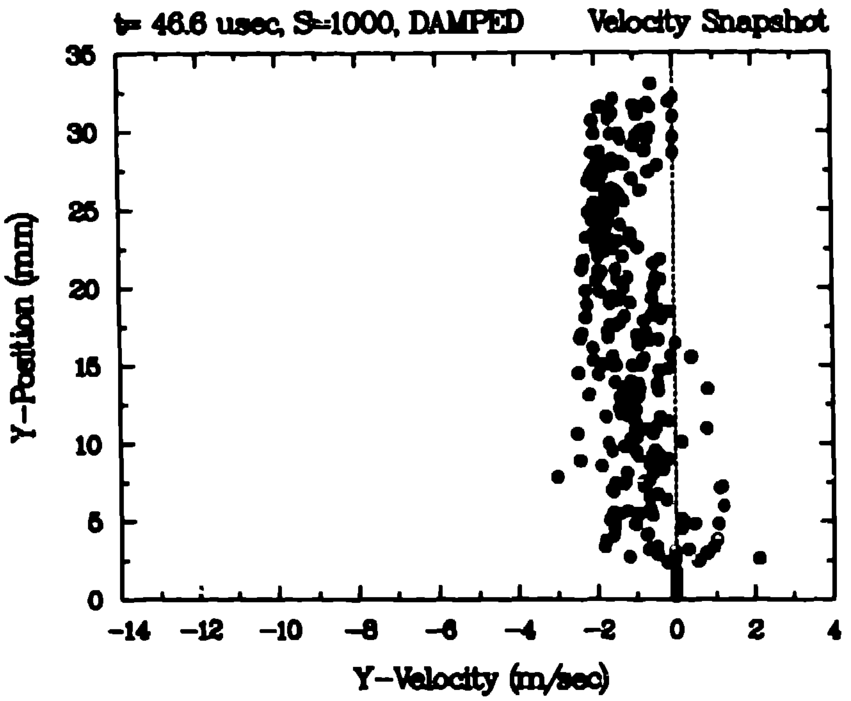

SKRUBAL SNAPSHOT

Fig. 7d.

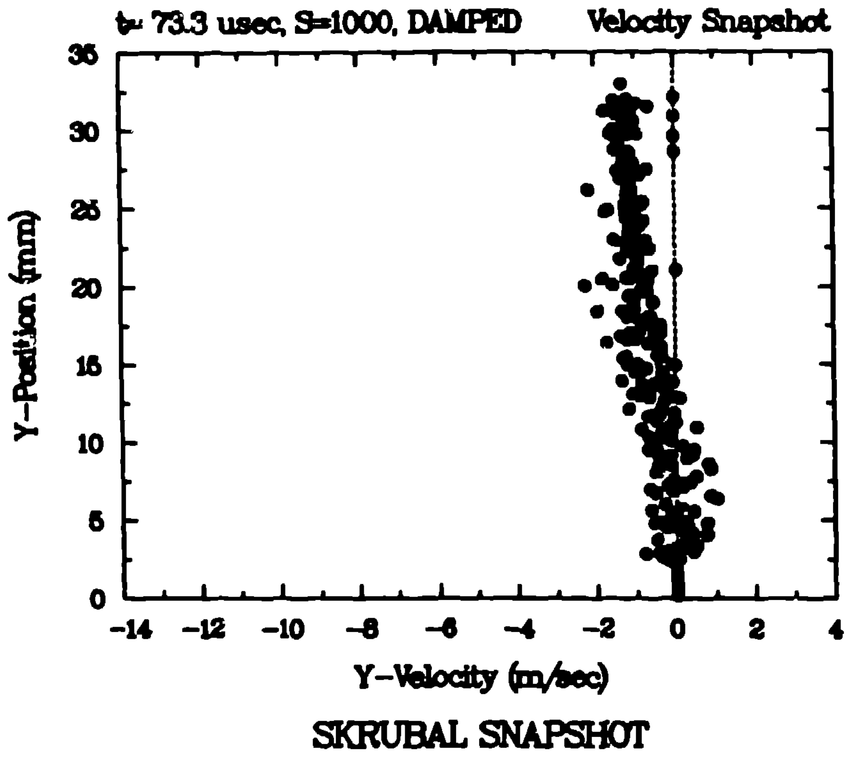
t= 73.3 usec, S=1000, DAMPED
Velocity Snapshot
Y-Position (mm)
Y-Velocity (m/sec)
35
30
25
20
15
10
5
0
-14
-12
-10
-8
-6
-4
-2
0
2
4
SKRUBAL SNAPSHOT

Fig. 7e.

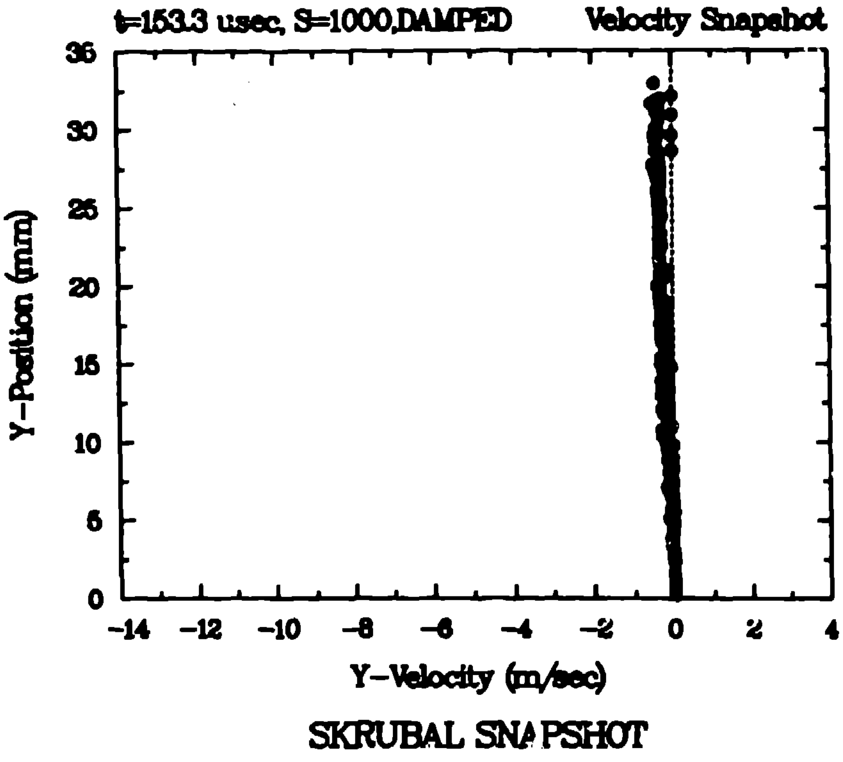
t=153.3 usec, S=1000,DAMPED
Velocity Snapshot
36
30
25
20
15
10
5
0
Y-Position (mm)
-14
-12
-10
-8
-6
-4
-2
0
2
4
Y-Velocity (m/sec)
SKRUBAL SNAPSHOT

Fig. 7f.

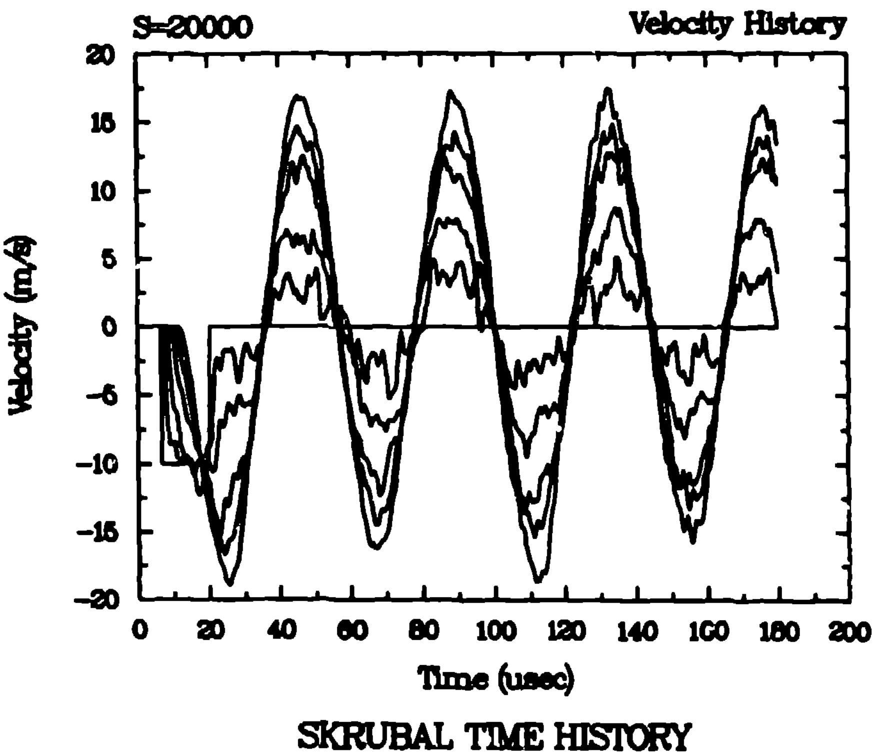

Fig. 8. Undamped wave propagation through the sample shown in Fig. 2. The elastic modulus is 20 GPa and the bonds are 95% intact. Sound speed is 1460 m/s.

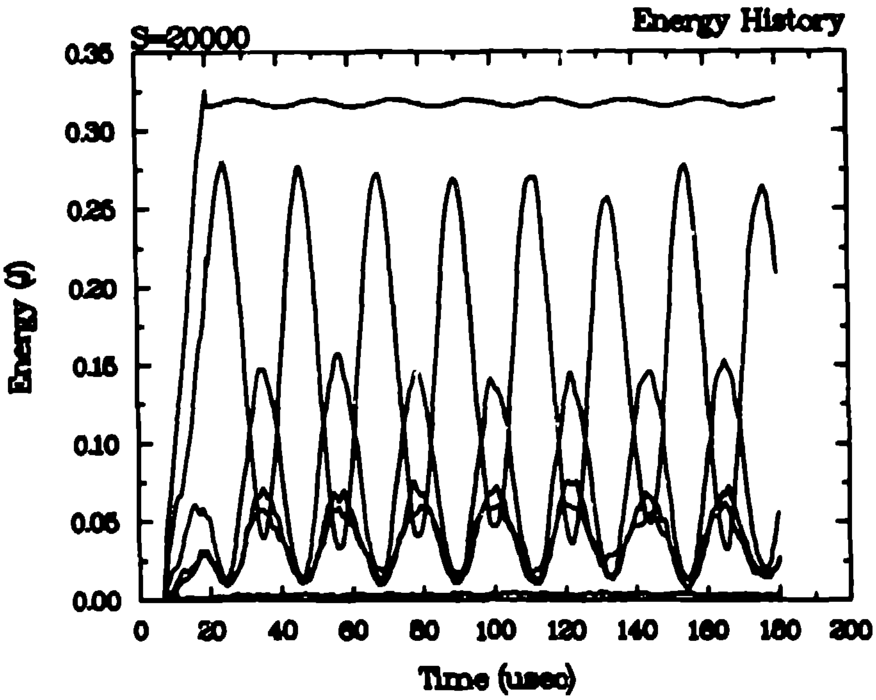

SKRUBAL TIME HISTORY

Fig. 9. Energy terms for the loading shown in Fig. 8. The upper curve is total energy and the curve with the greatest amplitude change is the translational kinetic energy in the particles. The other harmonic curves are the components of strain energy in the bonds which are greatest when particle motion is minimized. The energy stored during normal tension and compression of the bonds is the greatest while the strain energies in the rolling and shearing torsion modes are nearly equal. The lowest curve is the rotational kinetic energy of the particles.

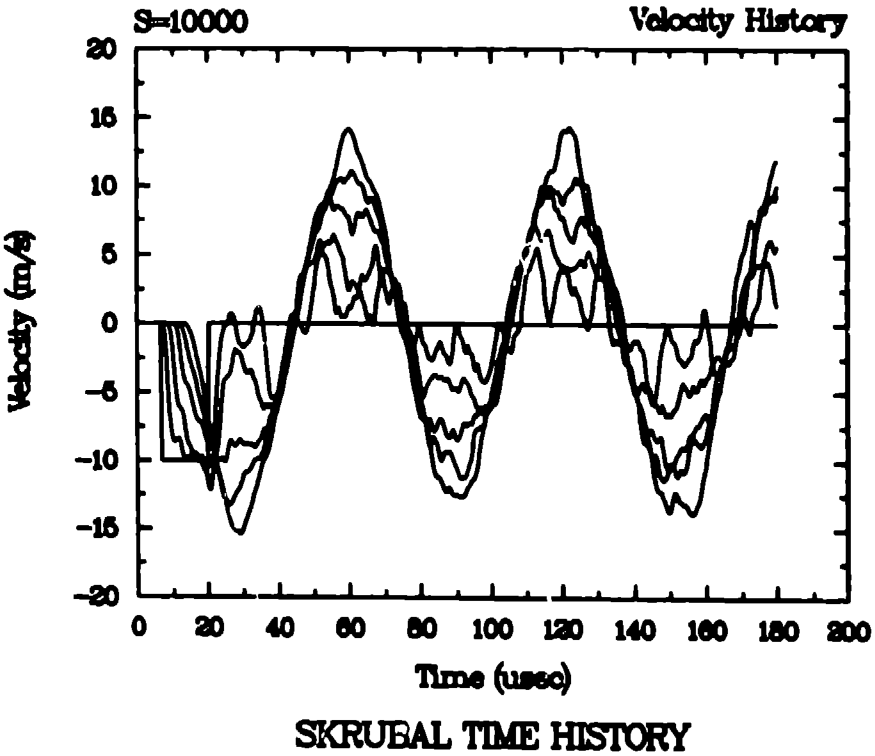

Fig. 10. Undamped response due to identical loading of the sample in Fig. 2 as before, except that the elastic modulus of the bonds has been decreased to 10 GPa. Sound speed is 1050 m/s.

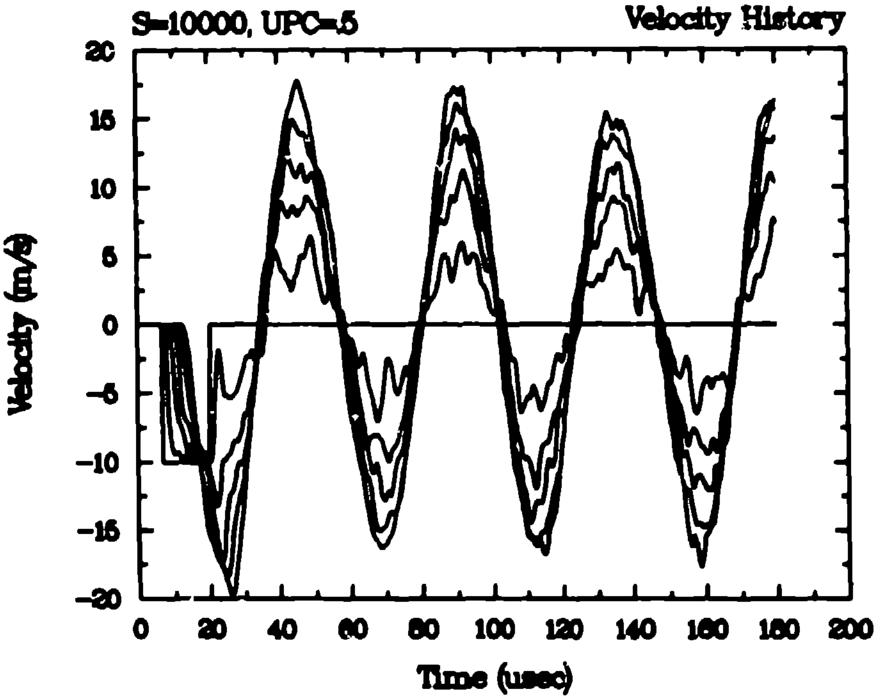

SKRUBAL TIME HISTORY

Fig. 11. Response of loading of the sample in Fig. 3. Elastic modulus of the bonds is 10 GPa, but the additional 83 bonds make the macroscopic response stiffer. Sound speed is 1440 m/s.

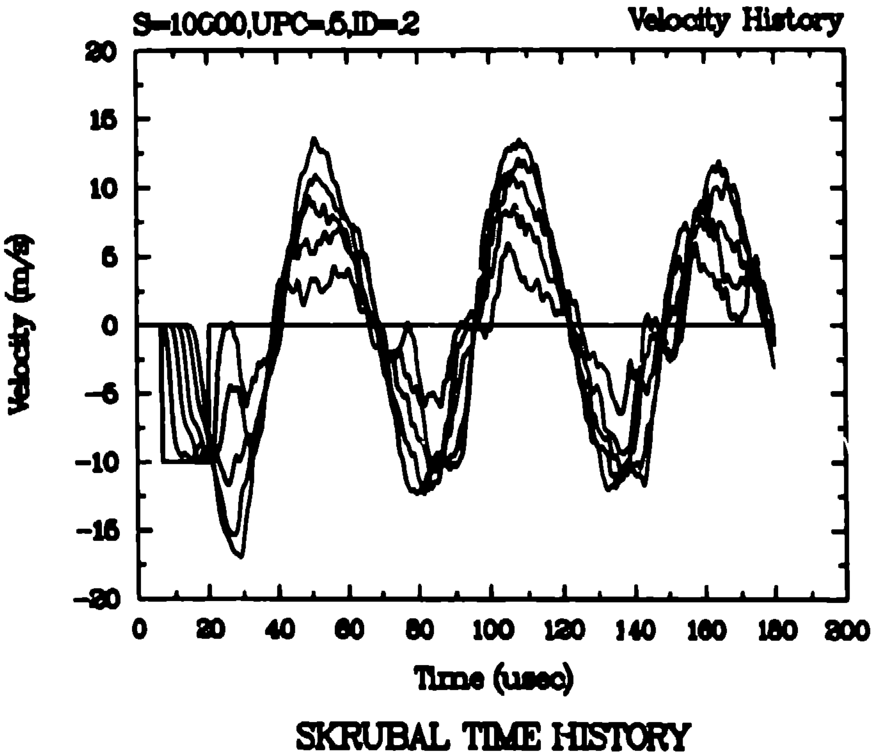

Fig. 12. Velocity time histories for the sample in Fig. 3. Here the bonds are only assumed to be 80% intact. The elastic modulus is 10 GPa and there are 480 bonds. Sound speed is 1150 m/s.